

Unusual magnetic properties of the heavy-fermion compound CeCoGe_3

V. K. Pecharsky,* O.-B. Hyun,[†] and K. A. Gschneidner, Jr.

Ames Laboratory and Department of Materials Science and Engineering, Iowa State University, Ames, Iowa 50011

(Received 3 August 1992; revised manuscript received 7 December 1992)

Heat capacity, magnetization, and electrical resistivity measurements were carried out on CeCoGe_3 and LaCoGe_3 . CeCoGe_3 was found to be a heavy-fermion system with $\gamma = 111$ mJ/mole Ce K^2 . Two magnetic transitions were found at ~ 21 and ~ 18 K in the absence of a magnetic field. The upper ordering temperature is believed to be a transition from the paramagnetic state to a c -axis ferrimagnetic (FERRI) state, which in turn transforms a colinear antiferromagnetic (AF) state at ~ 18 K. The AF phase undergoes an irreversible phase transition to the FERRI state under an applied magnetic field. Consequently, magnetic glasslike behaviors such as thermal and magnetic hysteresis, frozen moment, and magnetic relaxation were observed. A nonhysteretic metamagnetic transition to a c -axis ferromagnet (FERRO) was observed at high magnetic fields. The critical spin-flip field, H_m , increases in the FERRI state, and decreases in the AF state as temperature decreases. The magnetic data also suggest that the Ce moments in the ab plane are antiferromagnetically aligned in all three magnetic phases. The existence of both ferromagnetism and antiferromagnetism implies that there may be close competition of ferromagnetic and antiferromagnetic exchange interactions between Ce moments leading to possible spin frustration.

I. INTRODUCTION

In the course of our research on new intermetallic compounds in the $RT\text{Ge}_3$ system, where R represents rare earths and T represents transition metals, we have found some interesting magnetic properties in CeCoGe_3 . Both LaCoGe_3 and CeCoGe_3 crystallize in the body-centered BaNiSn_3 structure.¹ This structure is related to the ThCr_2Si_2 structure.² In the BaNiSn_3 unit cell, four of the Sn atoms replace the four Cr atoms, and the two Ni atoms plus two Sn atoms occupy in an ordered fashion the four Si atoms of the parent ThCr_2Si_2 unit cell, see Fig. 1.

CeCo_2Ge_2 , which has the ThCr_2Si_2 -type structure, is an intermediate valence compound with Kondo-like anomalies.³ There are three major differences in the structure of CeCoGe_3 compared to CeCo_2Ge_2 . One is the connectivity of the Ce-Co atoms in the c direction. In the CeCo_2Ge_2 phase, the four Co atoms on the faces in the upper half of the structure are connected to the body-centered Ce atom (at a distance of 3.256 Å) which, in turn, is connected to the four Co face atoms in the lower half of the structure [see Fig. 1(b)]. In the CeCoGe_3 phase, the four atoms on the edges in the upper half of the unit cell are connected to a single Co atom (at a distance of 3.414 Å which is connected to the body-centered Ce atom (at a distance of 3.391 Å) in the lower half of the unit cell [see Fig. 1(a)]. The second is a chain of atoms along the four-fold axis, which has the sequence Ce-Ge-Ge as the repeat unit in CeCo_2Ge_2 , while in CeCoGe_3 it is Ce-Co-Ge as the repeat unit. The third, which is a result of these two differences, is the absence of reflection symmetry along the fourfold (c) axis in CeCoGe_3 , while CeCo_2Ge_2 possesses a mirror plane. It should also be noted that the Ce-Ce and Ce-Co distances in CeCoGe_3

are ~ 7 and 5% larger, respectively, than in CeCo_2Ge_2 , which is reasonable since a large Ge atom is replacing a small Co atom. Furthermore, the shortest Co-Co distance is quite large in the BaNiSn_3 -type structure, and is equal to the a edge of the unit cell, 4.35 Å, which compares to 2.89 Å in CeCo_2Si_2 and 2.50 Å in pure Co. With these structural differences in mind, we thought that a detailed study of CeCoGe_3 might provide useful information on the relationship between structure and interatomic distances and the various types of behaviors found in Ce-containing materials, i.e., magnetic ordering, Kondo lattice, heavy fermion, mixed valence, etc.

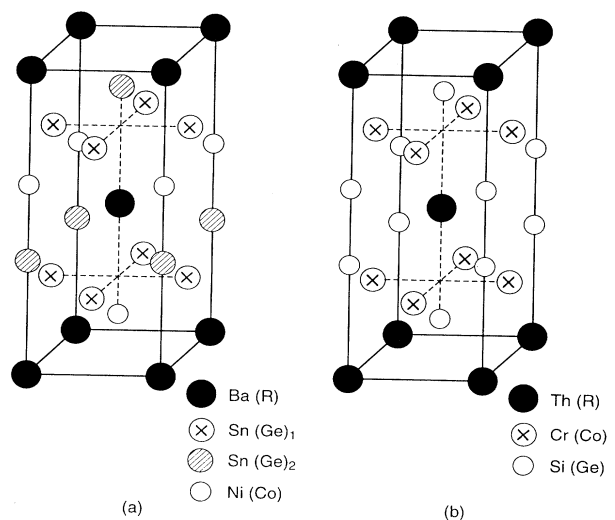


FIG. 1 (a) The BaNiSn_3 structure, and (b) the ThCr_2Si_2 structure. The symbol R represents Ce and La.

Unlike CeCu_2Si_2 and its isostructural compounds, there have been no extensive studies of the RTM_3 compounds. Among CeTM_3 compounds, there is a superconductor (CeCoSi_3) and Kondo lattice systems (CeRhSi_3 and CeIrSi_3) (Ref. 4) and a spin-glass system (CePtSi_3).⁵ The spin-glass property is particularly interesting since no chemical disorder was found in the system. Among nine RTGe_3 compounds examined ($R = \text{La, Ce, Pr, Nd, and Eu, and } T = \text{Co and Rh}$), the CeTGe_3 phases are found to be heavy-fermion systems.⁶ CeRhGe_3 shows unusual spin canting, for which the critical field of spin flip decreases as temperature decreases. In addition, the mixed quaternary systems $\text{CeCo}_{0.9}\text{Rh}_{0.1}\text{Ge}_3$ and $\text{Ce}_{0.8}\text{La}_{0.2}\text{CoGe}_3$ show spin-glass behavior.⁶ This suggests that there is high potential for some degree of frustration in CeCoGe_3 . In this paper, we present the results of the low-temperature, high-magnetic-field heat-capacity, magnetization, and resistance measurements on CeCoGe_3 .

II. EXPERIMENTAL DETAILS

The lanthanum and cerium used in this study were prepared by the Materials Preparation Center of the Ames Laboratory and were 99.79 at. % (the main impurities: H, 0.17; O, 0.02; and N, 0.01 at. %) and 99.93 at. % (the main impurities: O, 0.04 and C, 0.015 at. %) pure, respectively. The cobalt was purchased from Johnson Matthey Company, Ltd. (England) and the germanium from Cerac, Inc. Both were better than 99.999 wt % pure with respect to the metallic and semimetallic elements.

The alloys with nominal compositions LaCoGe_3 and CeCoGe_3 were prepared by arc melting pieces of metals under an argon atmosphere and then heat treating them at 900°C for 7 days in helium-filled quartz tubes. The weight losses after arc melting were less than 0.2% of total mass which was about 5 g for both samples, thus, the alloy compositions were assumed to be unchanged. Phase and crystal structure analyses were performed by means of metallography and room-temperature x-ray powder diffractometry (using a SCINTAG automated powder diffractometer, Cu $K\alpha$ graphite monochromated radiation).

Low-temperature zero-field (1.3–50 K) and magnetic (1.3–20 K) heat capacities up to 9.8 T were measured using an adiabatic heat-pulse-type calorimeter.⁷ The magnetic susceptibility was measured from 1.5 to 300 K in a 1.1 T field by using a Faraday microbalance.⁸ Magnetization data in applied fields up to 5.5 T were collected on a SQUID magnetometer.

The electrical resistance was measured using a standard four-probe dc technique. Data were taken with the current applied in each direction to eliminate possible thermal effects.

In addition to the usual polycrystalline samples, which are normally cut out or sometimes broken off of an ingot, two grain-aligned polycrystalline samples were prepared for magnetic measurements because CeCoGe_3 is strongly anisotropic with the easy axis parallel to the tetragonal axis. A polycrystal sample was thoroughly ground and

grain aligned in nonmagnetic epoxy (EPOTEK 301) by a magnetic field of 8.2 T. Two cylindrical samples were made for the magnetization measurements, one parallel and the other perpendicular to the c axis. The disalignment was checked by a rocking curve, which was found to be less than 2.5° of the (004) peak in FWHM. A small misalignment was observed mainly due to bicrystals.

III. RESULTS

A. Crystal structure and sample characterization

X-ray powder patterns indicated that both LaCoGe_3 and CeCoGe_3 crystallize in the BaNiSn_3 -type structure (Fig. 1). A least-squares fit of the data gave the lattice parameters and atomic positional parameters, which are listed in Table I. No apparent chemical disorder was found through a Rietveld refinement. The lattice parameters for the two compounds agree within the experimental error with the previous values reported by Venturini *et al.*¹ The x-ray-diffraction pattern gave no evidence for the presence of second phases. Optical metallography showed the presence of ~1% of a second phase (which could not be identified) and also revealed a uniform grain size between 10 and 30 μm .

B. Zero-field heat capacities

The heat capacities of LaCoGe_3 and CeCoGe_3 from ~1.5 to 30 K are shown in Fig. 2. The heat capacities of both samples were measured up to 50 K, but since the two curves remain essentially parallel to one another from 25 to 50 K, only the data below 30 K are shown. The parallelness of the two curves indicate that the lowest excited crystal-field level is greater than 100 K. If

TABLE I. Crystallographic data of LaCoGe_3 and CeCoGe_3 (space group $I4mm$).

	LaCoGe_3	CeCoGe_3
a (Å)	4.3497(2)	4.3192(2)
c (Å)	9.8679(4)	9.8298(2)
2θ range	26°–126°	26°–126°
Number of refl.	59	59
R	0.073	0.067
Atomic parameters		
R in (0,0, z)		
z	0.3361(2)	0.3344(2)
B_i (Å ²)	0.93(3)	0.80(2)
Co in (0,0, z)		
z	0.0000 ^a	0.0000 ^a
B_i (Å ²)	0.53(5)	0.76(5)
Ge 1 in (0,0, z)		
z	0.7702(3)	0.7707(2)
B_i (Å ²)	0.85(4)	0.51(4)
Ge 2 in (0,1/2, z)		
z	0.1008(2)	0.0985(2)
B_i (Å ²)	1.11(3)	1.06(3)

^aParameter kept fixed to determine origin in the space group.

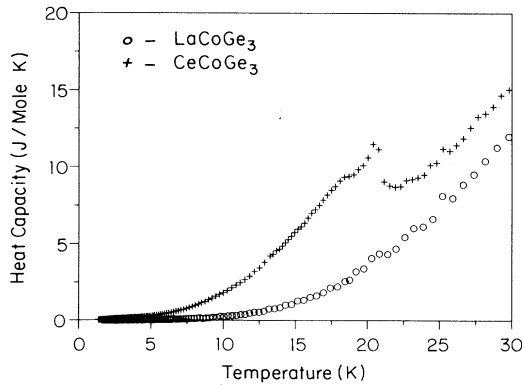


FIG. 2. The heat capacity of LaCoGe_3 and CeCoGe_3 from ~ 1.5 to 30 K.

the first level above ground state were less than 100 K, the curve for the Ce compound would pull away from the LaCoGe_3 curve toward higher heat-capacity values at approximately one-half of the crystal-field splitting (in K). The data given in Fig. 2 show a fairly sharp peak at 21.2 K and a broad shoulder at 18.5 K, which becomes more perceptible and looks like a rounded peak in a C/T vs T^2 plot (Fig. 3).

Not evident in Figs. 2 and 3 is a small peak at 2.8 K ($T^2 = 8 \text{ K}^2$), which is obvious in Fig. 4. The anomaly at 2.8 K was not studied any further. However, in view of the development of magnetic ordering in LaCoGe_3 due to the Co atoms (see below), it is possible that the Co atoms are also ordering in the CeCoGe_3 compound. The entropy under the peak amounts to only 1.0 mJ/mole K, which corresponds to 0.019% of the Co atoms per formula unit being involved in the ordering process assuming Co has an effective magnetic moment of $1.6\mu_B$. This is about the same number of Co atoms (0.013%) that are involved in the magnetic ordering of LaCoGe_3 as deduced from magnetization measurements at 5 K (see below).

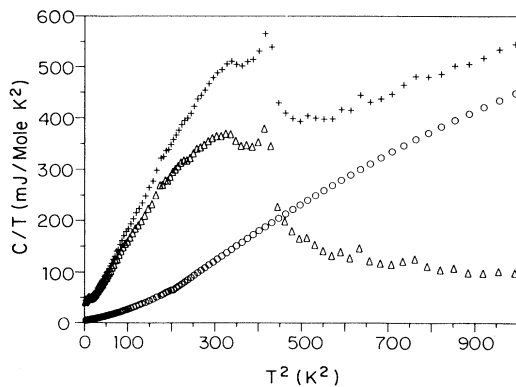


FIG. 3. A plot of C/T vs T^2 for LaCoGe_3 (\circ) and CeCoGe_3 ($+$), and the difference between the C/T values (Δ) of the two compounds from ~ 1.5 (2 K^2) to ~ 31.5 K (1000 K^2).

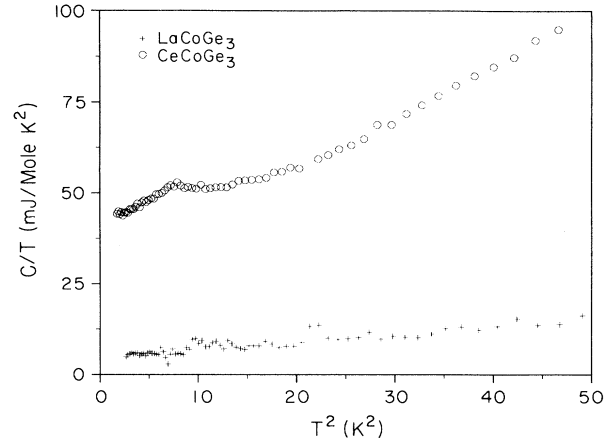


FIG. 4. The low-temperature portion of the C/T vs T^2 plot for LaCoGe_3 and CeCoGe_3 .

The electronic specific-heat constant, γ , and the Debye temperature, Θ_D , were obtained in the following manner for the two compounds and are listed in Table II along with some other values. The γ and Θ_D values for LaCoGe_3 were obtained from a least-squares fit of the C/T vs. T^2 data from ~ 1.5 to ~ 8.0 K (below $\sim 70 \text{ K}^2$), Fig. 4, which gives γ as the intercept and β as the slope. Θ_D is calculated from β using the relationship $\Theta_D^3 = (1.9437 \times 10^6)/\beta$, where β is in units of mJ/g at. K^4 , and Θ_D in K. Because of the magnetic ordering in the CeCoGe_3 compound one cannot use the same technique as for the La compound to obtain γ and Θ_D . Since the heat capacities of the two compounds maintain a constant C or C/T difference above ~ 25 K (see Figs. 2 and 3), we can determine the electronic specific constant of the Ce compound in excess of that of the La compound using the following expression:

$$\begin{aligned} \Delta(C/T) &= (C/T)_{\text{Ce}} - (C/T)_{\text{La}} \\ &= \gamma_{\text{Ce}} + \beta T^2 - (\gamma_{\text{La}} + \beta T^2) = \gamma_{\text{Ce}} - \gamma_{\text{La}}. \end{aligned}$$

This assumes that the lattice contribution for both $R\text{CoGe}_3$ compounds are the same, which is quite reason-

TABLE II. Some electronic, thermal, and magnetic properties of LaCoGe_3 and CeCoGe_3 .

Property	LaCoGe_3	CeCoGe_3
γ (mJ/mole R K ²)	4.92 ± 0.22	111
β (mJ/g at. K ⁴)	0.0431 ± 0.0016	
Θ_D (K)	356 ± 4	356^a
Parallel to c axis		
P_{eff} (μ_B)		2.43
θ_p (K)		-30.4
Perpendicular to c axis		
P_{eff} (μ_B)		2.48
θ_p (K)		-66.8

^aAssuming Θ_D to be the same as that of LaCoGe_3 .

able since the two phases have the same crystal structure, similar lattice parameters ($\Delta a=0.7\%$, $\Delta c=0.4\%$, and $\Delta V=1.8\%$) and are neighboring lanthanide elements with the same valence 3+, and a mass difference of 0.8%. A least-squares fit of the $\Delta C/T$ values (see Fig. 3) above 26.5 ($\sim 700 \text{ K}^2$) gives a $\gamma_{\text{Ce}}-\gamma_{\text{La}}$ value of 106 mJ/mole $R \text{ K}^2$, and thus $\gamma_{\text{Ce}}=111 \text{ mJ/mole Ce K}^2$, which suggests that this compound is a heavy-fermion material.

C. Magnetic-field heat capacity

The heat capacity of CeCoGe_3 near the magnetic ordering temperatures in magnetic fields up to 7.53 T is shown in Fig. 5. Below 13 K the heat capacity is independent of field. Between 13 and 18 K, the heat capacity appears to oscillate as the magnetic field is increased (see Fig. 5): first decreasing at $H=1.50 \text{ T}$, then rising, reaching the zero-field value at $H=2.46$, and continuing to rise above the zero-field values reaching a maximum at $H=5.32$, before falling back to the zero-field values at $H=7.53 \text{ T}$. The shoulder at $\sim 18 \text{ K}$ becomes less evident at $H=1.50$ and 2.46 T , and then disappears between $H=2.46$ and $H=5.32 \text{ T}$. This suggests that the high magnetic field destroys this magnetic state, shifting the magnetic entropy associated with this shoulder to higher temperatures. At the same time, the magnetic field shifts the 21.2 K upper magnetic transition to lower temperatures as is evident in Fig. 6; however, magnetic fields for $H > 5.3 \text{ T}$ do not shift the transition to lower temperatures. Unfortunately, our magnetic heat-capacity apparatus has an upper temperature limit of $\sim 21 \text{ K}$ and we are unable to study the heat capacity as a function of magnetic field at high temperature.

D. Electrical resistivity

The electrical resistivity of a polycrystalline CeCoGe_3 sample is shown in Fig. 7. The antiferromagnetic ordering is evident by the kink in the curve at $\sim 20 \text{ K}$, but there is no evidence of an anomaly or transition at either 18.5 or 2.8 K, which are the temperatures at which small

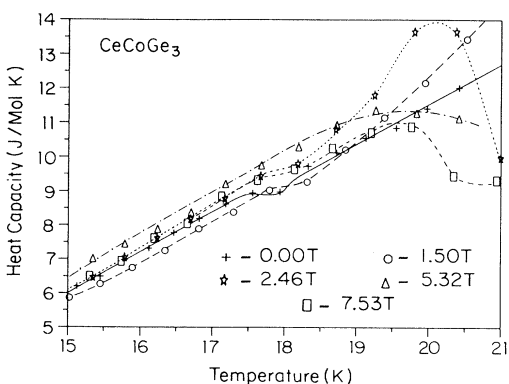


FIG. 5. The heat capacity of CeCoGe_3 at five magnetic fields between 15 and 21 K near the magnetic ordering temperatures. The various lines are guides for the eye.

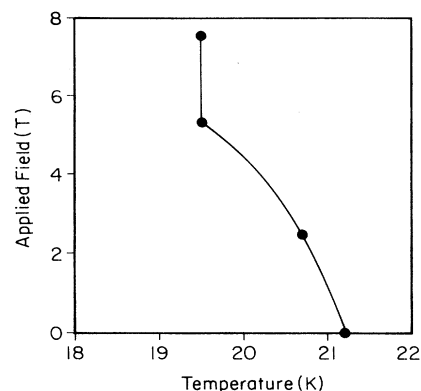


FIG. 6. The effect of magnetic field on the upper ordering temperature.

bumps are seen in the heat capacity (Figs. 2–4). Below 20 K the resistivity exhibits a quadratic temperature dependence, $R(T)=R_0+AT^2$, where $R_0=-0.017 \text{ m}\Omega$ and $A=2.31 \text{ m}\Omega/\text{K}^2$. This temperature dependence is consistent with magnetic ordering. Above 20 K the electrical resistivity increases as a function of temperature in a manner which is typical of a metallic material.

The magnetoresistance was also measured at 5 K as a function of magnetic field up to 5.5 (see inset, Fig. 7). The step and plateau in the resistance at $\sim 0.5 \text{ T}$ is consistent with a change in slope in the 3 K magnetization curve at this same field (see below, Fig. 12). Above about 1.5 T the resistance increases linearly with increasing magnetic field up to 3 T, and then it drops abruptly. This observation is consistent with a jump in the magnetization as a function of increasing magnetic field (see below, Fig. 12).

E. Magnetic measurements

The magnetic susceptibility was measured in a field of 1 T from 3 to 350 K. Above 100 K the data both parallel

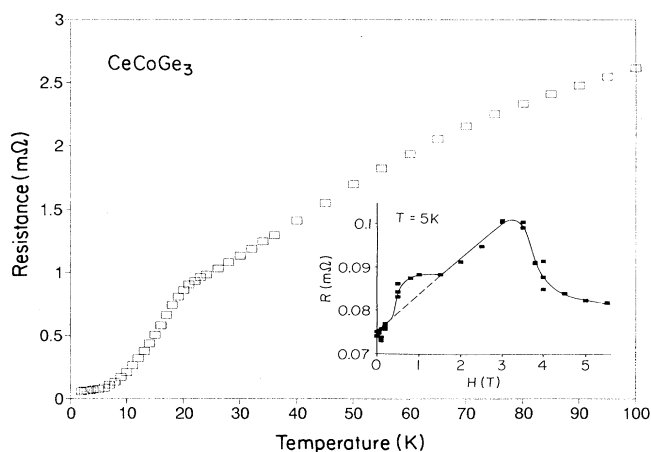


FIG. 7. Electrical resistance of CeCoGe_3 from 2 to 100 K. The inset shows the magnetoresistance at 5 K in magnetic fields up to 5 T.

and perpendicular to the c axis obeyed the Curie-Weiss (CW) law, see Fig. 8. The measured parameters—the effective magnetic moment, p_{eff} , and Curie-Weiss temperature, θ —are given in Table II. They indicate that Ce in this compound is essentially trivalent, the compound orders antiferromagnetically, and the compound is strongly anisotropic. It is interesting that p_{eff} for H perpendicular to the c axis is greater than that for H parallel to the c axis. The actual susceptibility, however, is greater along the c axis because of a smaller θ_p . The large negative values of θ for both directions implies that there may be strong antiferromagnetic ordering, particularly in the ab plane of the tetragonal structure. Below 60 K the inverse susceptibility, χ^{-1} , drops much faster than linearity as temperature decreases, i.e., a negative departure from the Curie-Weiss law behavior. This indicates a tendency toward ferromagnetism, that is, there are some weak ferromagnetic interactions in the presence of the dominant antiferromagnetic correlations. Since p_{eff} is close to that for $4f^1$, this would suggest that essentially all of the magnetic moment in this compound is carried by Ce, and that the d -band metal, Co, has no moment. This is confirmed by the fact that no appreciable Co moment was observed in the other isostructural $R\text{CoGe}_3$ compounds ($R=\text{La,Pr}$). There is, however, some evidence for a small Co moment in LaCoGe_3 (see below). The small Knight shift in CeCoGe_3 at low temperatures, 1.05% at 25 K and 0.42% at 10 K, also suggests the absence of a Co moment or at most a very small moment.

The magnetic susceptibility of LaCoGe_3 (Fig. 9) exhibits a nearly constant temperature-independent Pauli paramagnetism above ~ 50 K, but the rapid rise below 50 K suggests that some of the Co atoms may be tending to order, or that all the Co atoms are involved in the ordering process but the effective magnetic moment per atom is quite small. Thus, we measured the magnetization of the LaCoGe_3 sample at 70 and 5 K from 0 to 5.5 T. At 70 K the M vs H curve was linear and the intercept passed through zero, but at 5 K some curvature was observed indicating ferromagnetic ordering. Extrapolation of the high-field (4.5–5.5 T) magnetization data to $H=0$ gave a limiting off-set value of 0.0028 emu/g, which is

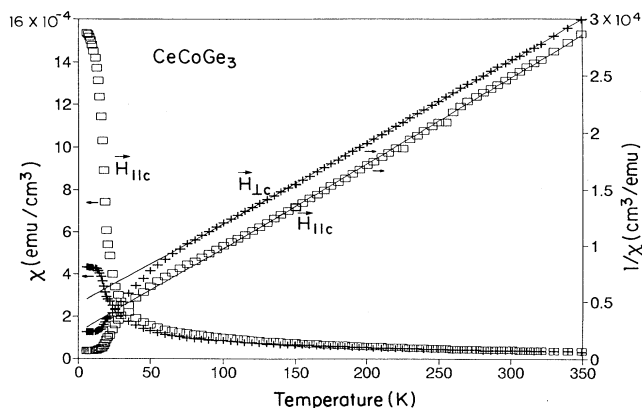


FIG. 8. Magnetic susceptibility of two oriented CeCoGe_3 polycrystalline samples from 3 to 350 K.

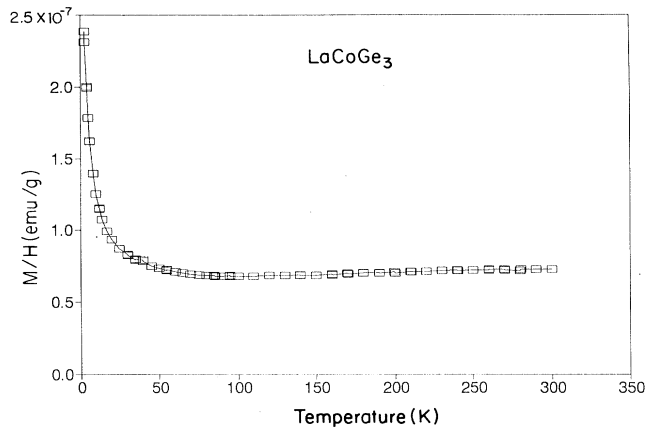


FIG. 9. Magnetic susceptibility of polycrystalline LaCoGe_3 from 3 to 300 K.

equivalent to an effective magnetic moment (p_{eff}) of $2.1 \times 10^{-4} \mu_B$ for the compound LaCoGe_3 . If the Co atoms that are involved in the ordering process had an effective moment of $1.6 \mu_B$, then the measured p_{eff} would be due to 0.013% of the Co atoms per formula unit. We believe that the ferromagnetic ordering involves all of the Co atoms, with each having a p_{eff} of $2.1 \times 10^{-4} \mu_B$, and that this is due to electron transfer from the La atom to Co to nearly fill the $3d$ bands. The magnetic ordering temperature has not been deduced from the magnetic measurements; however, the slight change in slope in the C/T vs T^2 plot (Fig. 3) at $T^2 \sim 200 \text{K}^2$ ($T \sim 14$ K) may be indicative of magnetic ordering, and is consistent with the magnetic data. The molar susceptibility of LaCoGe_3 from 50 to 300 K is 29.5×10^{-6} emu/mole. The behavior of this compound is quite similar to that found in $\text{LaCo}_{0.96}\text{Ge}_2$ except that the susceptibilities over the entire temperature range is about a factor of 4 times less in LaCoGe_3 than it is in $\text{LaCo}_{0.96}\text{Ge}_2$.⁹

We also considered the possibility that the small magnetic moment observed in the LaCoGe_3 (and also the small heat-capacity bump in CeCoGe_3) could be due to a few layers of metallic Co, which order at these low temperatures, on the surface of the samples. The formation of this Co surface layer could be a result of the oxidation of the LaCoGe_3 (or CeCoGe_3) to form La_2O_3 (or CeO_2), GeO_2 , and free Co. Au Auger analysis revealed that there was no free Co on the surface, and therefore the observed behaviors are most likely to be intrinsic to the $R\text{CoGe}_3$ materials.

We can also rule out the possibility that the susceptibility rise below 50 K is due to magnetic impurity atoms (other than Co) because of the high purity of the starting materials. The maximum magnetic impurity concentration in the lanthanum metal was 7.6 ppm atomic Fe, all other magnetic elements (both transition and lanthanide) were present at concentration levels < 0.5 ppm atomic; and that in the cobalt metal was 3 ppm atomic Ni and 1 ppm atomic Fe. A quick calculation shows that an iron content of about 42 ppm atomic would be required to account for the susceptibility rise observed in Fig. 9, which

is about five times larger than the sum of the measured iron concentrations in the starting materials. Similarly if the limiting off-set value from the 5 K magnetization data were due to iron impurities, 94-ppm atomic iron would need to be present in the LaCoGe_3 phase, which is about ten times larger than the observed iron content.

The temperature dependence of magnetization of CeCoGe_3 parallel to the c axis in a low field of 100 Oe under a variety of conditions is shown in Fig. 10, where a ferromagnetic-like increase below 20 K and gradual decrease of magnetization below 15 K as the temperature decreases is seen. Besides the difference between zero-field cooled (ZFC) (curve *a*) and field cooled (FC) either *b* or *c*) a remarkable recovery of the frozen moment measured at zero field after cooling is observed. A single magnetic phase with a ferromagnetic structure is not likely to explain the recovery, but the coexistence of two magnetic phases, a c -axis ferromagnet and a nonferromagnetic one, could explain the recovery of the frozen moment. The irreversibility temperature, where the ZFC magnetization splits from the FC magnetization, is 17 K at 100 Oe. This temperature is close to the zero-field heat-capacity shoulder (Figs. 2 and 3). The irreversibility temperature decreases with increasing field.

The high-field magnetization parallel to the c axis is shown in Fig. 11. For fields below 2 T a slight change in slope at ~ 20 K is evident and is consistent with the 21.2 K peak observed in the heat capacity (Fig. 2). The shapes of the magnetization vs temperature curves for $H < 2$ T is similar to that of a ferri- (or ferro-) magnetic material. Because the magnetization value at 1 T is about three times smaller than that at 4 T, we believe that at lower fields (< 2 T) CeCoGe_3 orders ferrimagnetically. When the magnetic field is increased ($H \geq 2.5$), a cusp develops at ~ 20 K which shifts to lower temperatures as H increases (similar to that observed in the heat-capacity results, see Figs. 5 and 6). This cusp is due to metamagne-

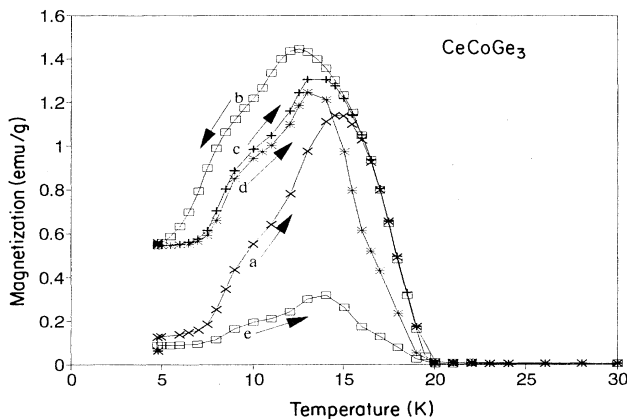


FIG. 10. Magnetization of CeCoGe_3 from 5 to 30 K for $H = 100$ Oe parallel to the c axis. (a) After ZFC. (b) FC with decreasing temperature (FCC). (c) FC with increasing temperature (FCW). (d) Same as (c) except with the field off. (e) FCW data for the 100-Oe magnetic field perpendicular to the c axis. The arrows indicate measurement directions in temperature.

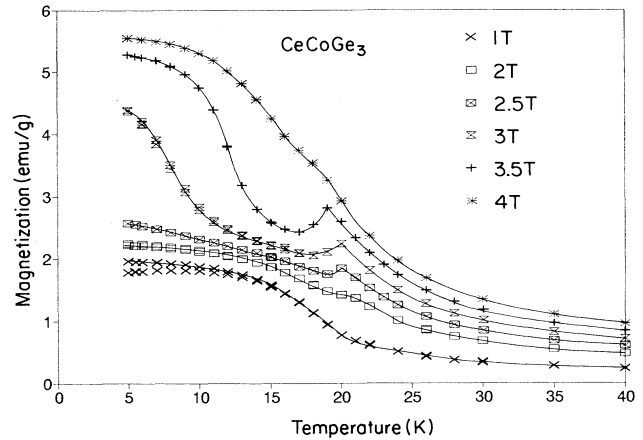


FIG. 11. Magnetization of CeCoGe_3 as a function of temperature at high magnetic fields with the magnetic field parallel to the c axis.

tism. For $H = 4$ T, the cusp is no longer observed and the magnetization vs temperature curve looks like that of a typical ferromagnetic material.

Magnetic isotherms were measured up to 5.5 T on both the parallel and perpendicular to c -axis samples. The magnetization is linear with the applied field for H perpendicular to the c axis at all temperatures. A typical curve ($T = 15$ K) is shown in Fig. 12. All isotherms below 20 K for the sample with the c axis aligned parallel to the magnetic field exhibited a metamagnetic transition due to spin flip at high fields. Magnetic hysteresis is observed below 15 K. At 3 K the coercive field is 800 G. The metamagnetic critical field, H_m , increases rapidly with decreasing temperature below 20 K, but quickly reaches a plateau at 15 K, and then slowly decreases as temperature decreases (see Fig. 13). The magnetization jump at H_m , ΔM , increases upon cooling as approximately $(1 - T/T_c)^{1/2}$ between 20 and 13 K, as expected from

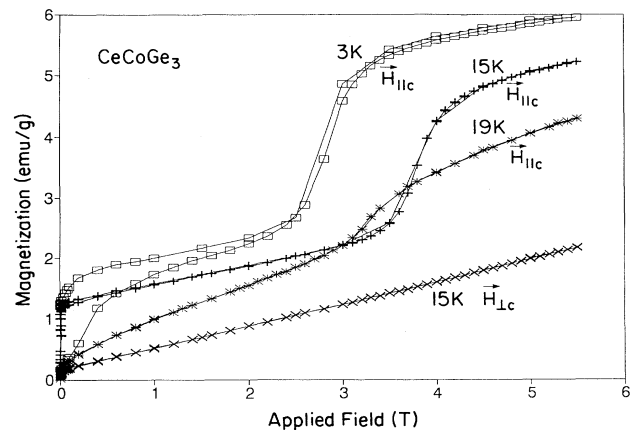


FIG. 12. Magnetization isotherms of CeCoGe_3 at 3, 15, and 19 K for H parallel to the c axis; and at 15 K for H perpendicular to the c axis.

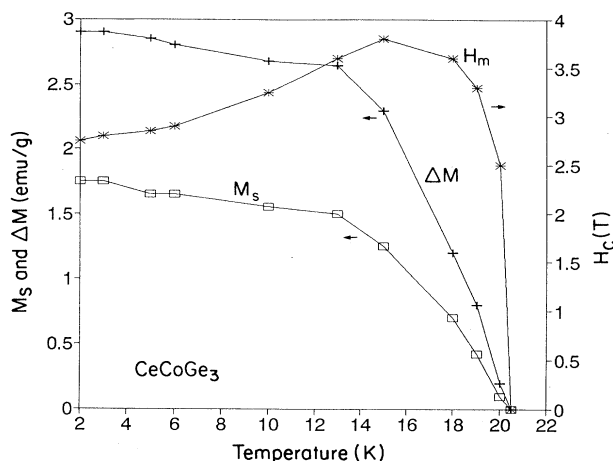


FIG. 13. The metamagnetic critical field, H_m ; the jump in magnetization at H_m , ΔM ; and the saturation magnetization, M_s ; for H parallel to the c axis as a function of temperature (see Fig. 12). The solid lines are guides to the eye.

mean-field theory (MFT).^{10,11} Below 13 K, however, the increase of ΔM is slower than expected from MFT. Since ferromagnetism above 15 K is nonhysteretic, we have extrapolated the linear part of isotherms to zero field to define M_s , which represents the longitudinal moment in the ferromagnetic state. As illustrated in Fig. 13, ΔM is approximately twice as large as M_s , suggesting a $++-+-$ ordering of the Ce moment along the c axis. Since M_s is about $0.12\mu_B$ at 3 K, the total longitudinal moment is found to be $0.37\mu_B$, which is much smaller than the full Ce moment ($2.14\mu_B$). Therefore, we believe that the Ce moments are primarily antiferromagnetically ordered in the ab plane, but are canted along the c axis. The canting order is $++-+-$, so that effectively only $\frac{1}{3}$ of the moments become saturated. Since the longitudinal component of the effective magnetic moment, $0.37\mu_B$, is only $\frac{1}{6}$ of the theoretical value ($g_J J = 2.14\mu_B$), a canting angle of about 10° from the ab plane would be needed to account for the observed c -axis magnetic moment. This canting sequence can be compared to that in CeAl_2Ga_2 which has the magnetic order $++-+-$ sequence of Ce moments along the c axis.¹² The Ce moment in CeAl_2Ga_2 was measured by neutron diffraction to be $1.3\mu_B$.¹² Because full c -axis ferromagnetism can be obtained above H_m , we have denoted the magnetic state between 15 and 20 K as c -axis ferrimagnetism.

IV. DISCUSSION

A. General

Judging from such facts as double peaks in the heat capacity, frozen moment recovery, and the increase and decrease of H_m , we believe that there are three distinct magnetic phases (see Fig. 14). Two are the c -axis ferromagnetic (FERRO) and the c -axis ferrimagnetic (FERRI) phases as described above. The third phase,

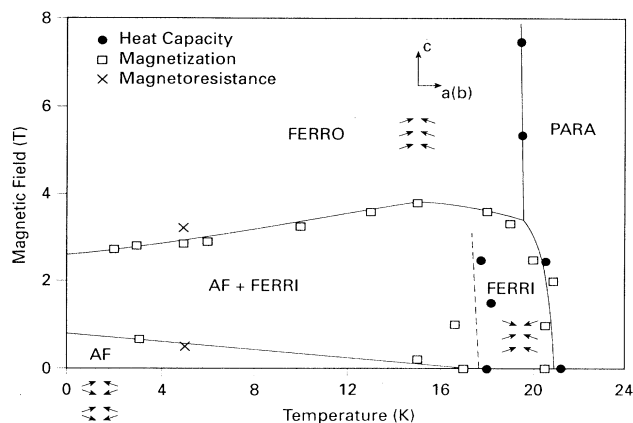


FIG. 14. Proposed magnetic phase diagram for CeCoGe_3 where PARA signifies the paramagnetic phase, FERRO the c -axis ferromagnetic phase, FERRI the c -axis ferrimagnetic phase, and AF the antiferromagnetic state. The arrows below the labels for the various magnetically ordered phases indicate the possible alignment of the magnetic moments on the Ce atoms with respect to the crystallographic orientation shown in the FERRO phase region. The various types of measurements used to deduce the phase boundaries are indicated in the figure by the various symbols.

which exists below 16 K, is a nonferromagnetic one. The phase transition from the nonferromagnetic to the FERRI phase is irreversible as seen in the isotherms (Fig. 12). We present two possible explanations, antiferromagnetic order and spin frustration.

B. Model I: Antiferromagnetic order

The first explanation is antiferromagnetic ordering of the Ce moment below 16 K. In this phase the c -axis ferrimagnetic order of the longitudinal component of the Ce moments changes to antiferromagnetic ordering as temperature decreases (see Fig. 14). More precisely, the canting order becomes $+-+-$, i.e., a collinear antiferromagnetic ordering along the c axis, which we denoted as AF. As temperature decreases from 16 K, small AF clusters appear and grow from the FERRI matrix. At lower temperatures AF becomes dominant while the FERRI phase remains as clusters or disappears completely. The FERRI clusters may be randomly oriented after ZFC. As temperature rises, FERRI clusters develop and grow, but are randomly oriented so that there is no magnetization from these clusters. Once the magnetic field is applied after ZFC, the favorably oriented clusters grow at the expense of others, and thus magnetization grows. After FC in low field, however, the magnetically induced FERRI phase competes and may coexist with thermodynamically favored AF, as shown by large magnetization in Fig. 10. Since all the FERRI clusters are oriented along the field direction in this case, the magnetization increases as FERRI clusters grow until thermal agitation becomes important above 16 K. Domain boundary pinning is believed to play a crucial role causing the thermal and magnetic hysteresis for this phase change. Unlike

the nonhysteretic FERRI state, the field-induced transition from AF to FERRI is not reversible because of domain-wall pinning. Also, AF is not fully recovered after the field is turned off for the same reason. The recovery is very slow as observed in the magnetization increase when the field is turned on after ZFC (Fig. 15). Energetically, the free energy of the AF phase is so close to that of FERRI state and the barrier between them is so low that even minor defects in the sample can interfere with the cluster motion by cluster wall pinning. Although the physics of the above picture, the closeness of the free energies of AF and FERRI phases, and the cluster wall pinning between them, is very different from that of a spin glass, both behaviors have similar outputs in magnetization, such as magnetic hysteresis, frozen moment, or relaxation. Neutron diffraction, however, should clearly distinguish the two behaviors.

C. Model II: Spin frustration

The second explanation is to describe the lower-temperature phase (below 16 K) as spin frustration (SF). In this scheme, the canting angle (or canting order) becomes random, resulting reentrant magnetic glass as in $\text{Au}_{1-x}\text{Fe}_x$ (with $16 < x < 24\%$).¹³ Alternatively, the Ce atoms may show a valence fluctuation such that long-range Ce^{3+} order no longer exists, resulting in spin frustration. The full Ce moment may be recovered at high field as demonstrated in TbMn_2 .¹⁴ In either case, the SF phase can be irreversibly destabilized to become the high-temperature FERRI phase.

D. Final comments

In either picture, FERRI-AF or FERRI-SF, close competition of ferromagnetic and antiferromagnetic exchange interactions between Ce moments are believed to be responsible for those magnetic orderings. The Ce-Ce interatomic distances are 4.319 Å for nearest neighbor (NN) and 5.787 Å for a next-nearest neighbor (NNN). These values are too large (even greater than in pure γ -Ce, 3.649 Å) to permit direct exchange interactions. In-

stead, long-range Ruderman-Kittel-Kasuya-Yosida (RKKY) interactions are believed to be dominant and responsible for the magnetic orderings in this compound. Based on these assumptions, we argue that spin frustration is not likely in this system without chemical disorder, which is not likely since a Rietveld refinement of the x-ray intensity data indicated all the atoms occupied the appropriate positions in the BaNiSn_3 structure. An important implication of *c*-axis ferrimagnetism and AF in CeCoGe_3 is provided by the absence of a SF phase and the presence of a colinear AF phase in UCu_2Ge_2 ,¹⁵ although it shows an irreversible magnetic phase transition from AF to ferromagnetism at low temperatures.

Increase and decrease of H_m in the FERRI and AF states, respectively, are not well understood. This type of H_m change has been reported in Tb-Ho alloys¹⁶⁻²¹ in which field-induced transition from helical magnetism to ferromagnetism was observed in the *ab* plane of the hexagonal structure. The critical field of the transition increases abruptly below T_N , then gradually decreases with decreasing temperature. The change was reported to coincide with an anomaly of thermal expansion coefficient and temperature dependence of the elastic constant, c_{44} . CeCoGe_3 , however, has two distinct magnetic phases and a different pattern of metamagnetism for each phase. The increase and decrease of H_m might imply lattice distortion at low temperature, which may induce different Dzyaloshinsky-Moryia^{22,23} (D-M) interactions in the magnetic phases. The decrease of H_m at low temperature was observed in another heavy-fermion CeRhCe_3 along the same axis.⁶

In order to determine which model is correct, neutron-diffraction studies as a function of magnetic field (up to 5 T) and temperatures below 25 K are needed, preferably on a single-crystal sample. Indeed it is possible that neither of the "simple" models is correct and the magnetic structures as a function of temperature and field are more complicated.

V. SUMMARY

We have found three magnetically ordered phases in CeCoGe_3 . At 20 K it shows a *c*-axis ferrimagnetism with ferromagnetic canting along the unique fourfold axis in the order of $++-+-$. Below 16 K, a colinear antiferromagnetic canting of the Ce^{3+} moments along the same axis is thought to occur. The low-temperature AF phase can be destabilized by a magnetic field to cause a transition into the high-temperature FERRI phase. The transition is hysteretic because of domain-wall pinning, causing magnetic spin-glass-like behavior. For all temperatures below 20 K, it becomes a *c*-axis ferromagnet (the third magnetic state) by a metamagnetic transition. The critical field of metamagnetism increases in a FERRI state, but decreases in an AF state, while the metamagnetic jump (the increase in magnetization at H_m) only increases as temperature decreases. In addition to the FERRI-AF explanation, the possibility of a FERRI-SF is also discussed. If CeCoGe_3 is a frustrated system, it might be related to the absence of a reflection symmetry in Ce-Co chains. Even if this is not a frustrat-

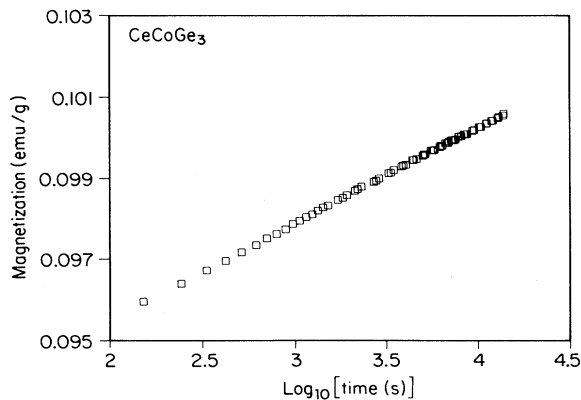


FIG. 15. Logarithmic time increase of magnetic moment at 5 K after ZFC to 5 K and then applying a magnetic field of 100 Oe.

ed system, a high potential for frustration exists due to the highly anisotropic symmetry.

ACKNOWLEDGMENTS

The authors thank D. C. Jiles and I. H. Kwon for valuable discussions, Y. D. Yoon for Knight shift measure-

ment at low temperatures, and A. J. Bevolo for carrying out the Auger analyses. Ames Laboratory is operated for the U.S. Department of Energy by Iowa State University under Contract No. W-7405-Eng-82. This work was supported by the Office of Basic Energy Sciences, U.S. Department of Energy.

*Permanent address: Department of Inorganic Chemistry, L'vov State University, L'vov, 290005, Ukraine.

†Present address: Superconductivity Research Laboratory, SRL in Japan Fine Ceramics Center, Nagoya, 457 Japan.

¹G. Venturini, M. Meot-Meyer, B. Malaman, and B. Roques, *J. Less-Common Met.* **113**, 197 (1985).

²W. Dörrscheidt and H. Schäfer, *J. Less-Common Met.* **58**, 209 (1978).

³H. Fujii, E. Ueda, Y. Uwatoko, and T. Shigeoka, *J. Magn. Magn. Mater.* **76**, 179 (1988).

⁴P. Haen, P. Lejay, B. Chevalier, B. Lloret, J. Etourneau, and M. Sera, *J. Less-Common Met.* **110**, 321 (1985).

⁵C. Geibel, C. Kämmerer, E. Göring, R. Moog, G. Sparn, R. Henseleit, G. Cordier, S. Horn, and F. Steglich, *J. Magn. Magn. Mater.* **90/91**, 435 (1990).

⁶O.-B. Hyun, V. K. Pecharsky, and K. A. Gschneidner, Jr. (unpublished).

⁷K. Ikeda, K. A. Gschneidner, Jr., B. J. Beaudry, and U. Atzmony, *Phys. Rev. B* **25**, 4604 (1982).

⁸R. J. Stiermann, K. A. Gschneidner, Jr., T.-W. E. Tsang, F. A. Schmidt, P. Klavins, R. N. Shelton, J. Queen, and S. Legvold, *J. Magn. Magn. Mater.* **32**, 4519 (1985).

⁹V. K. Pecharsky and K. A. Gschneidner, Jr., *Phys. Rev. B* **43**, 8238 (1991).

¹⁰A. S. Borovik-Romanov, *Zh. Eksp. Teor. Fiz.* **36**, 766 (1959) [*Sov. Phys. JETP* **9**, 539 (1959)].

¹¹A. S. Borovik-Romanov and V. I. Ozhogin, *Zh. Eksp. Teor. Fiz.* **39**, 27 (1961) [*Sov. Phys. JETP* **12**, 18 (1961)].

¹²D. Gignoux, D. Schmitt, M. Zerguine, E. Bauer, N. Pillonayr, J. Y. Henry, V. N. Nguyen, and J. Rossat-Mignod, *J. Magn. Magn. Mater.* **74**, 1 (1988).

¹³B. R. Coles, B. V. V. Sarkissian, and R. H. Taylor, *Philos. Mag. B* **37**, 489 (1978).

¹⁴R. Ballou, C. Lacroix, and M. D. Nunez Regueiro, *Phys. Rev. Lett.* **66**, 1910 (1991).

¹⁵J. Leciejewicz, L. Chelmski, and A. Zygmunt, *Solid State Commun.* **41**, 167 (1982).

¹⁶F. H. Spedding, R. G. Jordan, and R. W. Williams, *J. Chem. Phys.* **51**, 509 (1969).

¹⁷D. Fort, D. W. Jones, R. D. Greenough, and N. F. Hettiarachchi, *J. Magn. Magn. Mater.* **23**, 1 (1981).

¹⁸N. F. Hettiarachchi and R. D. Greenough, *J. Phys. C* **15**, 4573 (1982).

¹⁹P. de V. du Plessis, W. Botha, and G. H. F. Brits, *J. Magn. Magn. Mater.* **90/91**, 57 (1990).

²⁰R. Wendler, P. Pureur, A. Fert, and K. Baberschke, *J. Magn. Magn. Mater.* **45**, 185 (1984).

²¹B. Coqblin, *The Electronic Structure of Rare-Earth Metal and Alloys: The Magnetic Heavy Rare-Earths* (Academic, London, 1977).

²²E. Dzyaloshinsky, *J. Phys. Chem. Solids* **4**, 241 (1958).

²³T. Moriya, *Phys. Rev.* **120**, 91 (1960).